Interplay between density profile and zonal flows in drift kinetic simulations of slab ITG turbulence

Y. Sarazin 1), X. Garbet 1), V. Grandgirard 1), P. Bertrand 2), N. Besse 3), Ph. Ghendrih 1), E. Sonnendrücker 3)

1) Association Euratom-CEA, CEA/DSM/DRFC, Centre de Cadarache, 13108 Saint-Paul-Lez-Durance, France
2) LPMIA-Université Henri Poincaré Nancy I, Boulevard des Aiguillettes BP259, 54506 Vandœuvre-lès-Nancy, France
3) IRMA, CNRS-Université Louis Pasteur, 67084 Strasbourg, France

E-mail contact of main author: yanick.sarazin@cea.fr

Abstract. This paper reports on 4-dimensional drift kinetic simulations of the slab branch of the Ion Temperature Gradient driven turbulence in a cylinder. In the non-linear regime, the system is found to relax preferentially either via heat transport or via mean sheared flows, depending on the density profile. A strong density gradient appears to be stabilizing both linearly, by increasing the instability threshold, and non linearly, by activating sheared flows. This impedes the relaxation of the profiles and sustains a pressure transport barrier.

1. Introduction

It is now recognized that the magnitude of turbulent transport in magnetically confined plasmas is strongly governed by self generated zonal flows [1]. Such a back reaction could take the form of a random shearing of turbulent eddies, leading to a decrease of their mean size, and possibly to a reduced transport [2]. These flows are known to have a linearly undamped component in collisionless regimes [3]. In this framework, kinetic simulations are particularly well suited to investigate the mechanisms of their generation, as well as their impact on the transport.

The present paper investigates the interplay between the density gradient and the activity of zonal flows, and ultimately their impact on the turbulent transport level. This study is performed with a 4-dimensional drift-kinetic code for the slab branch of ion temperature gradient (ITG) driven turbulence. In agreement with previous works, the density gradient is found to linearly stabilize ITG modes by increasing the threshold. In addition, the simulations reported here show that a large density gradient is also stabilizing non-linearly, since it generates strong zonal flows, which tend to quench the turbulent transport.

2. Drift-kinetic model for the slab branch of ITG

A drift kinetic model is developed to investigate the slab branch of the ITG driven turbulence. The instability relies on the resonant interaction between waves and particles, namely parallel Landau resonances [4]. A periodic cylindrical plasma of radius a and longitudinal length $2\pi R$ is confined by a strong and uniform magnetic field $\mathbf{B} = B\,\mathbf{e_z}$. One considers the limit $k_\perp \rho_i << 1$, so that finite Larmor radius effects are neglected. In such a limit, the phase space reduces to 4-dimensions: the space coordinates (r,θ,z) and the parallel velocity $v_{//}$ along z. The electron response is taken adiabatic, but for equilibrium modes for which it vanishes. Within these approximations, the system is governed by two equations, the kinetic equation for the guiding-center ion distribution function f and the electro-neutrality constraint:

$$\partial_t f + D_B[\phi, f] + v_{//}\partial_z f - v_{T0}\,\partial_z \phi\,\partial_{v_{//}} f = 0 \qquad (1)$$

$$\frac{T_0}{T_e}\left(\phi - \langle\phi\rangle\right) - \rho_0^2\left\{\frac{n_0'}{n_0}\partial_r\phi + \Delta_\perp\phi\right\} = \frac{1}{n_0}\int f\, dv_{//} - 1 \qquad (2)$$

Here, ϕ denotes the normalized electric potential: $\phi = e\Phi/T_0$, where T_0 is a constant arbitrary temperature. D_B represents the so-called Bohm diffusion coefficient $D_B = T_0/eB = \rho_0 v_{T0}$, with $\rho_0 = m_i v_{T0}/eB$ the Larmor radius and $v_{T0} = (T_0/m_i)^{1/2}$ the thermal velocity. $\langle\phi\rangle$ is the potential averaged along the parallel direction z. The results presented here remain essentially unchanged when the average is performed on both periodic directions, namely z and θ. This should be emphasized in a forthcoming paper. Here, n_0 corresponds to the equilibrium particle density profile, while n_0' denotes its radial derivative. Poisson brackets come from the **E×B** advection term: $[\phi, f] = r^{-1}(\partial_\theta\phi\,\partial_r f - \partial_\theta f\,\partial_r\phi)$.

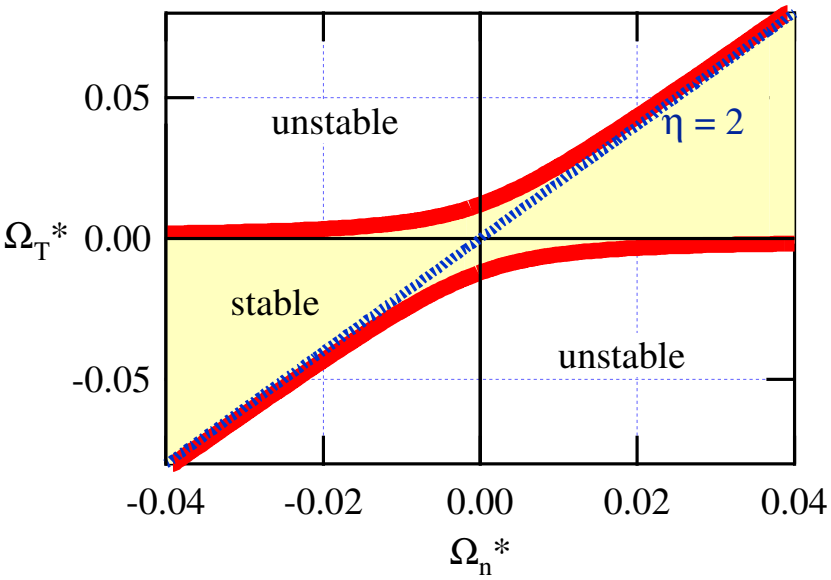

FIG. 1. Linear stability diagramme of the slab ITG model.

Perturbing a maxwellian equilibrium distribution function $f_{eq} = n_0 (2\pi T_{eq})^{-1/2} \exp(-E/T_{eq})$, the linear stability analysis of the system 1-2 gives a threshold. Looking at test functions for the mode profile of the form $\Phi_k = \phi_k\, exp[g(r)]$, the critical temperature gradient $A_T = T_{eq}'/T_{eq}$ is governed by the following equation:

$$\Omega_T^{*c} = \Omega_n^* \pm \left\{\Omega_n^{*2} + 4\omega_{//}^2\left(C^2 - C\right)\right\}^{1/2} \qquad (3)$$

The diamagnetic frequencies are: $\Omega_{n,T}^* = (k_\theta\rho_i)\, v_T\, A_{n,T}$, where the Larmor radius and the thermal velocity are $\rho_i = m_i v_T/eB$ and $v_T = (T_{eq}/m_i)^{1/2}$. The parallel frequency is $\omega_{//} = k_{//} v_T$, and C is defined by $C = 1 + \tau + (k_\theta\rho_i)^2 - \kappa(r)$, with $\kappa(r) = \rho_i^2\{(A_n + r^{-1} + g')g' + g''\}$. The stability diagramme is shown on figure 1. There are two distinct unstable regions, for positive and negative diamagnetic frequencies Ω_T^*. Large density gradients are stabilizing. In the limit of large density gradients $\Omega_n^* \to \pm\infty$, the threshold reduces to the usual condition $\eta^c = \Omega_T^{*c}/\Omega_n^* > 2$. Let us consider the fluid limit $\omega >> \omega_{//}$ of the mode frequency in the small density gradient case, namely for $|A_n/A_T| << (\omega_{//}/\omega)^2$. At leading order, and using the approximation $C \approx 1 + \tau$, the unstable branch is:

$$\omega = \frac{1+i\sqrt{3}}{2}\left|\frac{\omega_{//}^2 \Omega_T^*}{\tau}\right|^{1/3} \qquad (4)$$

Note that, in the fluid limit, the growth rate increases as the cubic root of the temperature gradient A_T.

3. Transport barrier vs. iso-thermal regimes

The system eqs.1-2 is solved numerically on a fixed grid in the phase space for the entire distribution function using a semi-Lagrangian scheme [5]. Details of the code named GYSELA can be found elsewhere [6]. Its accuracy is such that the number of particles and the energy are typically conserved within less than one percent in the non-linear regime. The initial profiles of density and T_i are essentially hyperbolic tangents, while T_e is constant. The driving force of the system consists of different densities and ion temperatures at the boundaries. Since the electrons are taken adiabatic, there is no net particle flux in the system. As a consequence, the particle density profile n_0 is constant in time. Conversely, the guiding center density profile $\langle n_G \rangle = \langle \int f \, dv_{//} \rangle$ may evolve since it relates to the radial derivative of the mean poloidal velocity $\langle v_\theta \rangle = D_B \partial_r \langle \phi \rangle$, namely the vorticity: $\langle n_G \rangle = n_0 - (1/\omega_c r)\, \partial_r \{ r n_0 \langle v_\theta \rangle \}$, where $\omega_c = eB/m_i$. The initial condition is such that $\langle n_G \rangle = n_0$.

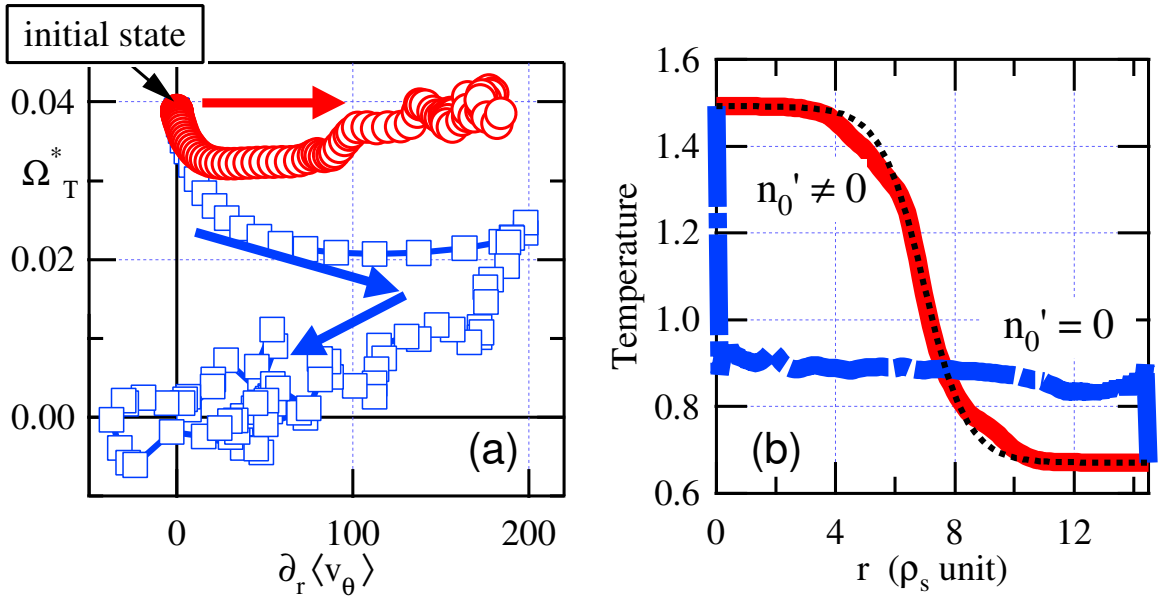

FIG. 2. Trajectories at mid radius for an initially flat (squares) or shaped (circles) density profile. Arrows indicate time evolution. (b) Temperature profiles in the turbulent regime for each case. The dotted line is the initial T_i profile.

Two cases with different initial conditions are compared. The trajectories of the central radial point of the system are plotted on figure 2a in a $(\langle v_\theta \rangle', \Omega_T^*)$ space. Circles refer to a finite initial density gradient. Square symbols correspond to the same case with a flat density profile. The central region is initially unstable in both cases. The flat density case relaxes towards marginality by decreasing the temperature gradient. The system is first subject to a transient activity of zonal flows, before they are almost quenched in the final state. A strong heat outflow at the beginning of the non-linear phase leads to an almost flat T_i profile, with strong gradients at the edges, as shown on figure 2b. In the other case, a mean sheared flow

$\langle v_\theta \rangle$ is self generated, leading to a transport barrier on the temperature profile. Such a back reaction of turbulence generated velocity shear on transport is indeed expected theoretically [2]. It is also instructive to plot the trajectory followed by the system in the plane $(\Omega_{nG}^*, \Omega_T^*)$, with Ω_{nG}^* computed from the guiding-center density profile n_G. In this case, the time evolution of Ω_{nG}^* mimics that of the velocity shear $\langle v_\theta \rangle'$. Figure 3 shows that, whatever density gradient, the system moves towards the linearly stable domain. However, the path which is followed differs significantly, ranging from an almost vertical to a horizontal displacement, depending on whether $n_0'=0$ or not, respectively.

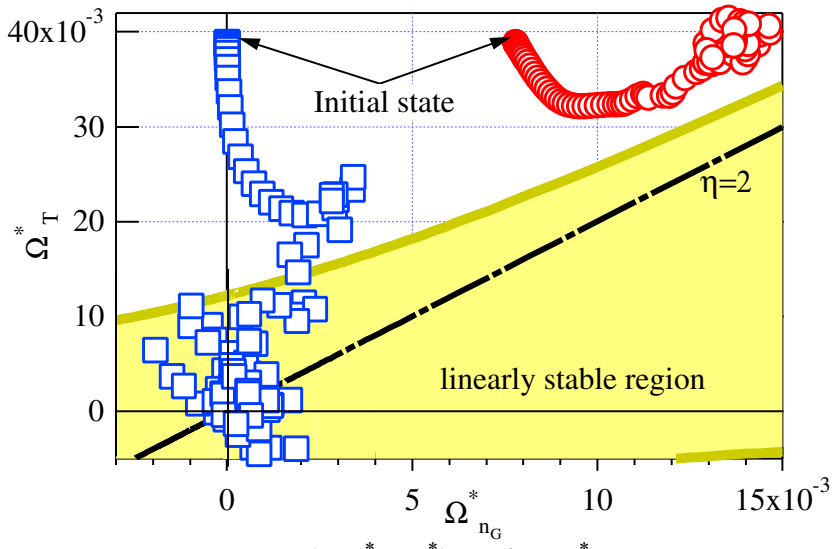

FIG. 3. Same as figure 2a in the plane $(\Omega_{nG}^*, \Omega_T^*)$, with Ω_{nG}^* computed from the guiding-center density profile n_G.

Figure 4 highlights the differences in the potential structure of the two simulations: while streamer-like convective cells develop when starting from a flat density profile, annular cells, characteristic of zonal modes, dominate for an initially shaped density profile. The multipolar radial structure of the velocity shear is reminiscent of the one reported in Particle In Cell simulations of the toroidal ITG instability [7].

4. Discussion

This section analyses the drastic dependence of zonal flow activity on the density profile. Let Γ be the flux of guiding-centers: $\Gamma = -(D_B/r)\ \langle n_G\ \partial_\theta \phi \rangle$. The first moment of the kinetic equation is such that the velocity shear of the zonal flows is governed by this flux:

$$\frac{\partial \langle v_\theta \rangle}{\partial t} = \omega_c \frac{\Gamma}{n_0} \tag{5}$$

In the absence of guiding-center flux Γ, there is no source for zonal flows. It is worth noticing the RHS of eq.5 can also be written in terms of the Reynolds stress tensor $\Pi = \langle \delta v_r\ \delta v_\theta \rangle = -D_B^2\ \Sigma_k\ k_\theta\ Im(\Phi_k^*\ \partial_r \Phi_k)$:

$$\omega_c \Gamma = -\frac{1}{r^2}\frac{\partial}{\partial r}\left(r^2 n_0 \Pi\right) \tag{6}$$

For a non-vanishing magnetic shear, like in tokamaks, an additional source/sink for zonal flows is to be taken into account, driven by geodesic acoustic modes [8].

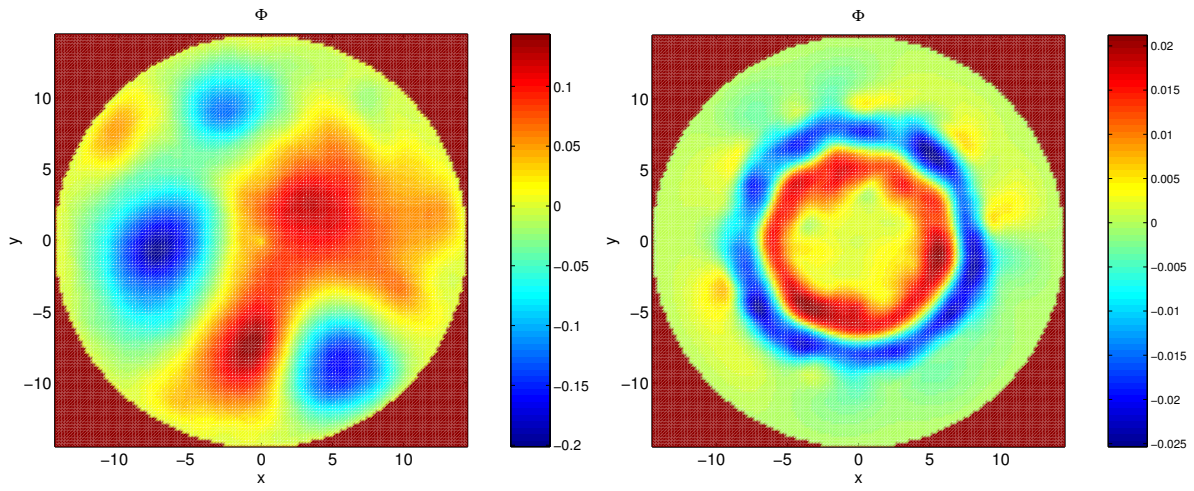

FIG. 4. Snapshot of the electric potential $\phi(r,\theta,z_0)$ at a given azimuthal position z_0 in the case where (a) $dn_0/dr \neq 0$ and (b) $dn_0/dr = 0$.

Further insight on the link between the density gradient and the generation of zonal flows requires the explicit expression of the Reynolds stress. We shall consider the quasi-linear expression of Π in the fluid limit. Let us consider the case of a mode developing close to the maximum of the temperature gradient, at the radius r_0. The density gradient is assumed to remain weak, more precisely $|A_n/A_T| << (\omega_{//}/\omega)^2$. The Taylor expansion in $x = r-r_0$ of the various profiles is then performed, the subscript *"0"* referring to the position $x=0$. These modes, that are solution of the linearized electro-neutrality eq.2, are gaussians of the form: $\Phi_k = \phi_k \exp\{-[(x-x^*)/\lambda]^2 / 2\}$. In this case, Π is proportional to the imaginary part of x^*/λ^2. Neglecting the terms in $\partial_r \Phi_k$ (valid for $r_0 A_{T0} >> 1$), simple expressions of x^* and λ can be derived. To leading order, and dropping high order derivatives, they read:

$$\frac{1}{\lambda^4} \approx \frac{\tau A_{T0}^2}{\rho_{i0}^2} - i\frac{\sqrt{3}}{2}\frac{k_\theta \omega_c A_{n0}^3}{|\omega|} \tag{7}$$

$$x^* \approx \frac{1}{2A_{T0}} - i\frac{\sqrt{3}}{4}\frac{k_\theta \rho_{i0} v_{T0} A_{n0}^2}{\tau|\omega| A_{T0}^2} \tag{8}$$

Here, the mode frequency ω has been replaced by its expression in the fluid limit, eq.4. The Reynolds stress then reads:

$$\Pi = -\frac{\sqrt{3} D_B^2}{4\tau^{1/2}} \sum_{k_\theta, k_{//}} k_\theta^2 \left|\Phi_k\right|^2 \frac{v_{T0}}{|\omega|} \frac{A_{n0}^2}{A_{T0}} \tag{9}$$

Π turns out to be proportional to the density gradient square, namely $A_{n0}^2 = (n_0'/n_0)^2$. As a result, the Reynolds stress vanishes if the density profile is flat. This is consistent with the numerical results discussed previously, where zonal flows are dominating the non-linear regime only for the shaped density case.

5. Conclusion

In summary, the system relaxes preferentially either via heat transport or via mean sheared flows, depending on the density profile. A strong density gradient appears to be stabilizing both linearly, by increasing the instability threshold, and non linearly, by activating sheared flows. A quasi-linear analysis in the fluid limit suggests that the latter mechanism could be due to the proportionality of the Reynolds stress with the gradients of the density profile. Such a back reaction of density gradients on turbulence provides a means to sustain pressure transport barriers.

References

[1] Hammett G.W., Beer M.A., Dorland W., Cowley S.C., Smith S.A., Plasma Phys. Control. Fusion **35**, 973 (1993); Sydora R.D., Decyck V.K., Dawson J.M., Plasma Phys. Control. Fusion **38**, A281 (1996); Lin Z., Hahm T.S., Lee W.W., Tang W.M., White R.B., Science **281**, 1835 (1998); Terry P.W., Rev. Mod. Phys. **72**, 109 (2000)

[2] Diamond P.H., Rosenbluth M.R., Hinton F.L., Malkov M., Fleisher J., Smolyakov A., Plasma Phys. Control. Nucl. Fusion Res. (IAEA, Vienna, 1998)

[3] Rosenbluth M.N., Hinton F.L., Phys. Rev. Lett. **80**, 724 (1998)

[4] Coppi B., Rosenbluth M.R., Sagdeev R.Z., Phys. Fluids **10**, 582 (1967)

[5] Cheng C.Z. and Knorr G., J. Comp. Phys. **22**, 330 (1976)

[6] Grandgirard V., Brunetti M., Bertrand P., Besse N., Garbet X., Ghendrih Ph., Manfredi G., Sarazin Y., Sauter O., Sonnendrücker E., Vaclavik J., Villard L., submitted to J. Comp. Phys. (2004)

[7] Villard L., Allfrey S.J., Bottino A., Brunetti M., Falchetto G.L., Grandgirard V., Hatzky R., Nührenberg J., Peeters A.G., Sauter O., Sorge S., Vaclavik J., Nucl. Fusion **44**, 172 (2004)

[8] Hallatschek K., Biskamp D., Phys. Rev. Lett. **86**, 1223 (2001)